

See discussions, stats, and author profiles for this publication at: <https://www.researchgate.net/publication/263959026>

Structural Chemistry of Oximes

ARTICLE in CRYSTAL GROWTH & DESIGN · MAY 2013

Impact Factor: 4.89 · DOI: 10.1021/cg4005246

CITATIONS

5

READS

19

6 AUTHORS, INCLUDING:



Abhijeet Sinha

University College Cork

10 PUBLICATIONS 46 CITATIONS

SEE PROFILE



Kanishka Epa

6 PUBLICATIONS 54 CITATIONS

SEE PROFILE



Michelle Smith

8 PUBLICATIONS 167 CITATIONS

SEE PROFILE

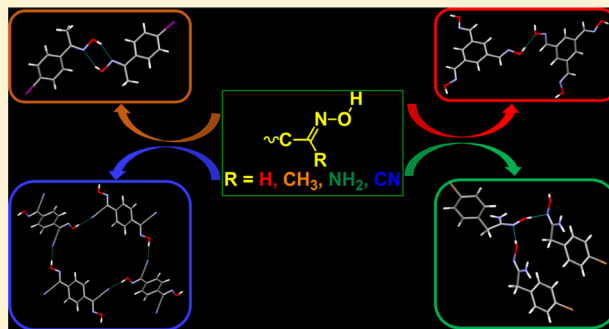
Structural Chemistry of Oximes

Christer B. Aakeröy,* Abhijeet S. Sinha, Kanishka N. Epa, Prashant D. Chopade, Michelle M. Smith, and John Desper

Department of Chemistry, Kansas State University, Manhattan, Kansas 66506, United States

Supporting Information

ABSTRACT: Oximes ($RR'C=N-OH$) represent an important class of organic compounds with a wide range of practical applications, but a systematic examination of the structural chemistry of such compounds has so far not been carried out. Herein, we report a systematic analysis of intermolecular homomeric oxime...oxime interactions, and identify hydrogen-bond patterns for four major categories of oximes ($R' = -H, -CH_3, -NH_2, -CN$), based on all available structural data in the CSD, complemented by six new relevant crystal structures. The structural behavior of oximes examined here, can be divided into four groups depending on which type of predominant oxime...oxime interactions they present in the solid-state: (i) $O-H\cdots N$ dimers ($R_2^2(6)$), (ii) $O-H\cdots N$ catemers ($C(3)$), (iii) $O-H\cdots O$ catemers ($C(2)$), and (iv) oximes in which the R' group accepts a hydrogen bond from the oxime moiety catemers ($C(6)$). The electronic and structural effects of the substituent (R') on the resulting assembly has been explored in detail to rationalize the connection between molecular structure and supramolecular assembly.

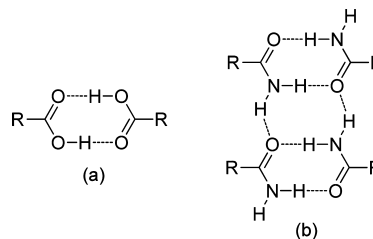


1. INTRODUCTION

The unparalleled success of synthetic organic chemistry¹ is directly related to the predictable chemical reactivity that is associated with well-known functional groups, such as aldehydes, esters, amines, etc. The targeted assembly of desired solid-state architectures² or of multicomponent crystals with predetermined stoichiometry and metrics³ similarly requires detailed information about the structural preferences and patterns of behavior that can be expected from specific chemical functionalities.^{4,5} Consequently, to advance crystal engineering to a higher level of complexity, the structural chemistry of key functional groups such as acids ($R_2^2(8)$ motif),^{6–8} amides ($C(4)R_2^2(8)$ motifs)^{7,9} and phenols ($C(2)$ chains)¹⁰ have been systematically examined and subsequently established to such an extent that confident predictions can be made as to how such entities are likely to self-assemble in the solid-state (Scheme 1).⁴

Oximes are well-known,^{11,12} easily accessible¹² and ubiquitous in both research laboratories and in large-scale production,^{13,14} and studies focusing on the structural aspects of some oximes have been presented. Hydrogen-bond patterns in crystalline oximes have been analyzed by Bertolasi et al.,¹⁵ followed by a systematic examination of hydrogen-bonding in aromatic and aliphatic oximes by Bruton et al.¹⁶ More recently, a review by Low et al. examined hydrogen-bonding patterns in aldoximes, ketoximes, and O-alkylated ketoximes, with and without competing acceptors (other acceptors than the oxime nitrogen atom).¹⁷ This study outlined the different hydrogen-bonding motifs present, and the effect of competing acceptors on the assembly of these motifs for aldoximes and ketoximes.

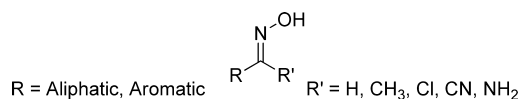
Scheme 1. (a) Hydrogen-Bonded $R_2^2(8)$ Dimer in Carboxylic Acids and (b) Hydrogen-Bonded infinite $C(4)R_2^2(8)$ Ribbons in Amides



However, a systematic, side-by-side, investigation of the structural chemistry of the most common and important members of the oxime family, has not yet been presented.

Oximes have the general formula $RR'C=N-OH$ (Scheme 2), and since they can act as both a weak acid ($pK_a \approx 11$) and a weak base ($pK_b \approx 12$), the oxime anions tend to be ambident in nature and, thus, can be used for the synthesis of different

Scheme 2. Different Types of Oximes



Received: April 9, 2013

Revised: May 8, 2013

Published: May 9, 2013



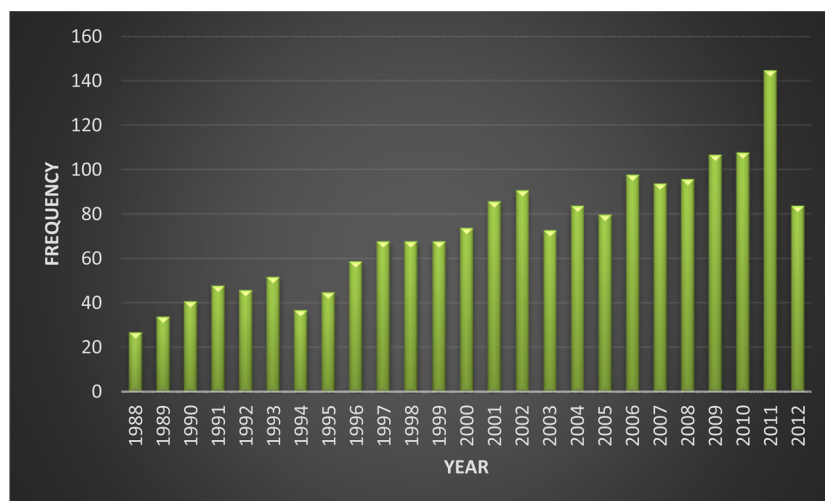


Figure 1. Number of reported crystal structures for oximes ($R' = -H, -CH_3, -NH_2, -CN$), 1988–2012.

compounds such as oxime ethers¹⁴ or nitrones.¹⁴ They have also been used in the characterization, purification and protection of functionalities such as aldehydes and ketones.¹⁸ Also, oximes upon deprotonation, can act as strongly coordinating ligands in metal-coordination chemistry.¹⁹

The literature on the structural chemistry of oxime-containing compounds is prolific, as shown by an examination of the Cambridge Structural Database (CSD);^{20,21} the four most common types of oximes ($R' = -H, -CH_3, -NH_2, -CN$) give a total of 2392 hits, of which 592 are organic substances. The wide interest in this chemical functionality is further illustrated by the fact that there has been an increased interest in their synthesis and applications over the past few years (Figure 1). In addition, as the previous cumbersome solution-based methods¹⁸ of synthesis of oximes are likely to be replaced by more versatile routes including green and robust mechanochemical pathways,^{22,23} the use and importance of oximes are likely to continue to grow.

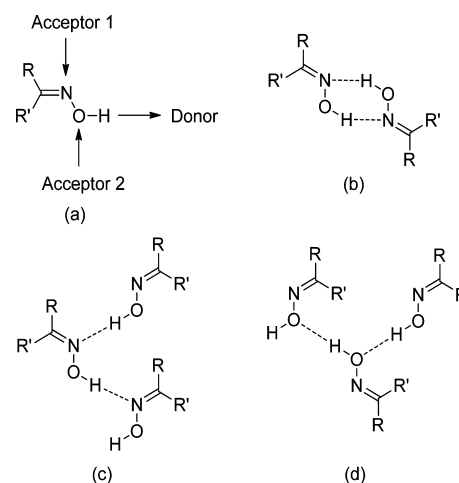
Oximes can act as both hydrogen-bond donors (via the $-O-H$ moiety) and as hydrogen-bond acceptors (via the $-C=N$ and the $-OH$ moieties) and thus can form dimers, as well as oxime...oxime catemers via $O-H\cdots N=C$ and $O-H\cdots OH$ hydrogen-bonds in the solid-state (Scheme 3).¹⁵ Also, the substituents (R') such as $H_2N-/N\equiv C-$ moieties, may influence the structural chemistry of such oximes in the solid-state via $O-H\cdots NH_2$ and $O-H\cdots N\equiv C$ interactions (Scheme 4).

Despite the ever increasing number of crystallographic studies of oximes, their structural chemistry has not been investigated in detail and their behavioral patterns in solid-state has not yet been clearly established. In this paper, we will classify the hydrogen-bonded intermolecular oxime...oxime interactions and try to establish patterns of behavior of the four major categories of oximes ($R' = -H, -CH_3, -NH_2, -CN$) (Scheme 5), by analyzing the available solid-state data in the CSD, complemented by six new crystal structures. We also will investigate the possible structural or electronic effects that govern the binding preferences of oximes as a function of R' group.

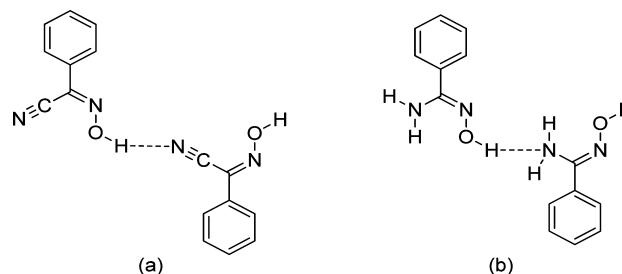
2. EXPERIMENTAL SECTION

All chemicals, unless otherwise noted, were purchased from Aldrich and used without further purification. Melting points were determined

Scheme 3. (a) Hydrogen-Bond Donor/Acceptors in Oximes, (b) Hydrogen-Bonded Dimers, (c) Catemer Formation via $-O-H\cdots N$ Hydrogen-Bonded Chains, and (d) Catemer Formation via $-O-H\cdots O$ Hydrogen-Bonded Chains



Scheme 4. (a) Hydrogen-Bonded Chains via $O-H\cdots N\equiv C$ Interactions in Cyano-Oximes and (b) Hydrogen-Bonded Chains via $O-H\cdots NH_2$ Interactions in Amidoximes



on a Fisher-Johns melting point apparatus and are uncorrected. The single-crystal growth conditions and melting points of all compounds are given in Table 1.

2.1. CSD Search. Oxime...oxime intermolecular interactions were mined from data in the CSD using four different searches (Scheme 6). Search 1 in the CSD on the four major types of oximes ($R' = -H, -CH_3, -NH_2, -CN$), gives data that show oxime...oxime $O-H\cdots N$ hydrogen bonds, whereas search 2 gives all the $O-H\cdots N$ hydrogen-

Scheme 5. Four Major Categories of Oximes Examined in This Study

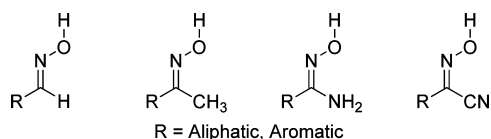
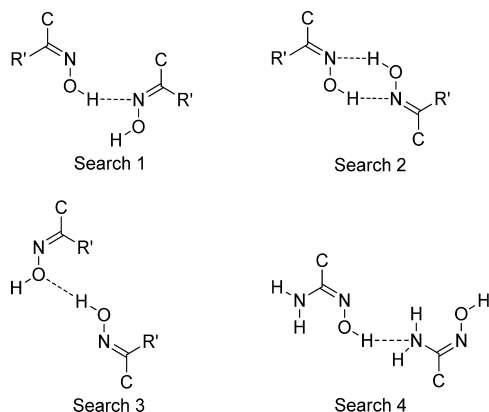


Table 1. Single-Crystal Growth Details and Melting Points of 1–6

compound	solvent for crystal growth	observed melting point (°C)	literature melting point (°C)
4-iodobenzaldehyde oxime (1)	ethyl acetate	100–102	101–103 ²²
4-cyanoacetophenone oxime (2)	ethyl acetate	150–153	150–153 ²³
4-bromoacetophenone oxime (3)	methanol	126–129	128–130 ²⁴
4-iodoacetophenone oxime (4)	ethyl acetate	156–160	156–158 ²⁵
(z)-2-(4-bromophenyl)-N'-hydroxyacetimidamide (5)	methanol	127–130 ^a	133–135 ²⁶
1,4-bis(cyanooximinomethyl)benzene (6)	water	240–247 (dec.)	

^aThe melting point for three individual crystallites of 5 was determined, for which we have reported a single-crystal structure, and it consistently came out to be 127–130 °C.

Scheme 6. Defined Parameters in the CSD during the Search for Data on Oximes



bonded dimers. The difference between the data sets of search 1 and 2 represents the catemers produced by O–H...N hydrogen-bonds. Search 3 finds O–H...O hydrogen-bonded catemers, whereas search 4 finds the O–H...NH₂ chains found in amidoximes. To focus on oxime...oxime interactions in the solid-state, all inorganic substances, salts, and cocrystals have been excluded from the search, and N/O heterocycles, α -carbonyl substituted oximes and solvates have been excluded, as they can act as hydrogen-bond acceptors and donors and thus disrupt oxime...oxime interactions. In addition, as we are focusing on oxime...oxime intermolecular interactions, all 1,2-disubstituted bisoximes have been excluded, as they are more prone to intramolecular hydrogen-bonded motifs. We have also complemented the existing CSD data by adding six new crystal structures.

2.2. X-ray Crystallography. Data sets were collected on a Bruker SMART APEX II system with Mo radiation (1, 2, 4, 5, 6) or a Bruker Kappa APEX II system with Mo radiation (3) at 120 K using APEX2 software.²⁷ An Oxford Cryostream 700 low-temperature device was used to control temperature. Initial cell constants were found by small

widely separated “matrix” runs. Data collection strategies were determined using COSMO.²⁸ Scan speeds and scan widths were chosen based on scattering power and peak rocking curves. Unit cell constants and orientation matrices were improved by least-squares refinement of reflections thresholded from the entire data set. Integrations were performed with SAINT,²⁹ using these improved unit cells as a starting point. Precise unit cell constants were calculated in SAINT from the final merged data sets. Lorenz and polarization corrections were applied. Where appropriate, absorption corrections were applied using SADABS.³⁰ Data sets were reduced with SHELXTL.³¹ The structures were solved by direct methods without incident. Unless noted below, the hydrogen atoms were assigned to idealized positions and were allowed to ride. Isotropic thermal parameters for the hydrogen atoms were constrained to be 1.2× that of the connected atom (1.5× that of the connected atom for –CH₃ groups). The coordinates for the oxime hydrogen atom H17 were allowed to refine for 1 and 2. In case of 3 and 4, the asymmetric unit contains two oxime molecules, and the coordinates for the oxime hydrogen atoms H17 and H27 were allowed to refine. In case of 5, the coordinates for the amine hydrogen atoms H22A and H22B, and for the oxime hydrogen atom H23 were allowed to refine. The molecule crystallizes in the noncentrosymmetric space group *P*2₁, where the choice of the correct absolute configuration was confirmed by a Flack parameter of 0.038(9). The coordinates for the unique oxime hydrogen atom H17 were allowed to refine for 6, where the molecule sits on a crystallographic inversion center.

2.3. Molecular Electrostatic Potential Calculations. Charge calculations were performed using Spartan'04 (Wave Function, Inc. Irvine, CA). All molecules were geometry optimized using DFT B3LYP/6-31+G* ab initio calculations, with the maxima and minima in the electrostatic potential surface (0.002 e au^{−1} iso-surface) determined using a positive point charge in vacuum as a probe.

3. RESULTS

Depending upon the presence of different acceptors and donors in oximes, the intermolecular interactions between two or more oximes in the solid-state can be classified into four major categories: (i) dimers based on –O–H...N hydrogen bonds (*R*₂²(6) motif), (ii) catemers directed by –O–H...N interactions (C(3) chains), (iii) catemers governed by –O–H...O hydrogen bonds (C(2) chains), and (iv) oximes in which the R' group plays a dominant role by accepting a hydrogen-bond from the oxime moiety (C(6) catemeric chains).

3.1. Aldoximes (R' = H). An examination of the crystal structure of 1 reveals that hydrogen-bond donors (the –OH moieties) are engaged in –O–H...N intermolecular interactions with oxime nitrogen atoms (the C=N moiety) of neighboring molecules (O17...N17 2.839(2) Å, O17–H17...N17 2.08(3) Å), thus forming dimers (Figure 2). Individual dimers are interconnected via halogen bonds between an iodine atom of one molecule and the lone pair of an oxygen atom of an adjacent molecule, which indicates that these are electrostatically driven interactions. The C–I...O

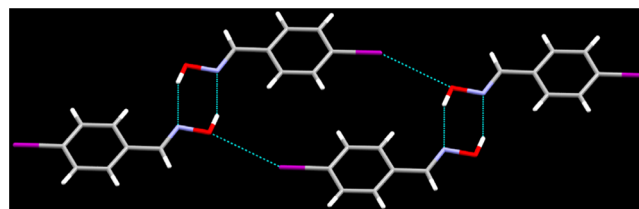


Figure 2. Section of the crystal structure of 1 displaying the hydrogen-bonded *R*₂²(6) dimer and an I...O halogen bond.

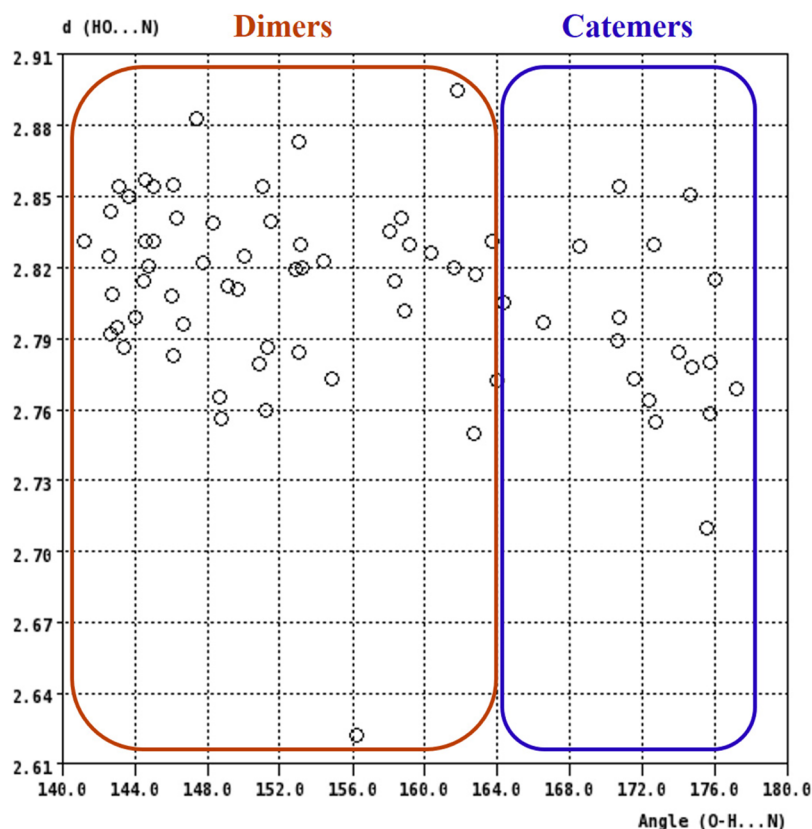


Figure 3. HO...N bond distance (Å) vs O-H...N bond angle (deg) for dimers and catemers of aldoximes.

bond angle is $154.74(5)^\circ$, and the O...I bond distance is $3.4471(15)$ Å.

There is a total of 58 crystal structures of aldoximes in the CSD, 42 of which form hydrogen-bonded dimers via $\text{O}-\text{H}\cdots\text{N}$ interactions (average HO...N bond distance and O-H...N bond angle is $2.82(4)$ Å and $150(7)^\circ$, respectively) (Figure 3). There are fourteen aldoximes in which catemer formation is directed by $\text{O}-\text{H}\cdots\text{N}$ interactions (average HO...N bond distance and O-H...N bond angle is $2.79(4)$ Å and $171(5)^\circ$ respectively), and in two aldoximes the primary interactions are $\text{O}-\text{H}\cdots\text{O}$ hydrogen-bonds leading to catemers. In summary, 72% aldoximes exist as dimers, 24% as catemers with $\text{O}-\text{H}\cdots\text{N}$ interactions, and 4% display $\text{O}-\text{H}\cdots\text{O}$ hydrogen-bonded catemers.

3.2. Ketoximes ($\text{R}' = \text{CH}_3$). The crystal structure determination of **2** showed dimers constructed from $\text{O}-\text{H}\cdots\text{N}$ interactions between adjacent oxime molecules with an HO...N bond distance of $2.7614(14)$ Å (Figure 4) (Table 2).

The crystal structures of **3** and **4** show identical features to those displayed by **1**. Again, the primary motifs are $\text{O}-\text{H}\cdots\text{N}$ hydrogen-bond based dimers with the HO...N bond distances

for **3** and **4** of $2.8379(16)$ Å ($\text{O}27\cdots\text{N}17$), and $2.813(3)$ Å ($\text{O}27\cdots\text{N}17$), respectively (Table 2). In both **3** and **4**, neighboring dimers are connected via $\text{C}-\text{X}\cdots\text{O}$ halogen bonds where the $\text{X}\cdots\text{O}$ bond distance for **3** and **4** are $3.0664(10)$ Å and $3.1727(17)$ Å, respectively (Figure 5) (Table 2). Another notable observation for **3** and **4**, is the presence of a pseudo-2-fold rotation axis that relates the two asymmetric units.

The search for single-component ketoximes in the CSD generated 37 crystal structures, 32 (87%) of which are dimers governed by $\text{O}-\text{H}\cdots\text{N}$ hydrogen bonds (average HO...N bond distance and O-H...N bond angle is $2.81(3)$ Å and $154(9)^\circ$, respectively) (Figure 6). Five (13%) ketoximes exist as catemers directed by $\text{O}-\text{H}\cdots\text{N}$ interactions (average HO...N bond distance and O-H...N bond angle is $2.81(6)$ Å and $172(5)^\circ$, respectively), whereas none of the ketoximes contain intermolecular $\text{O}-\text{H}\cdots\text{O}$ hydrogen bonds.

3.3. Amidoximes ($\text{R}' = \text{NH}_2$). The crystal structure determination of **5** reveals three interesting features. First, the $=\text{N}-\text{O}-\text{H}$ group on one oxime interacts with the $=\text{N}-\text{O}-\text{H}$ moiety on two adjacent oxime molecules via $\text{O}-\text{H}\cdots\text{N}$ hydrogen bonds leading to catemers ($\text{O}23\cdots\text{N}23$ $2.816(2)$ Å, $\text{O}23-\text{H}23\cdots\text{N}23$ $2.06(3)$ Å, $\text{O}23-\text{H}23\cdots\text{N}23$ $178(3)^\circ$) (Figure 7). Second, the polarizable bromine atom forms an intermolecular halogen bond with the oxygen atom on a neighboring oxime molecule, with an $\text{C}-\text{Br}\cdots\text{O}$ bond angle of $161.39(7)^\circ$ and an $\text{Br}\cdots\text{O}$ bond distance of $3.0902(16)$ Å, which underscores the electrostatic nature of this contact. Last, the assembly is extended by $\text{N}-\text{H}\cdots\text{N}$ hydrogen bonds between $-\text{NH}_2$ moieties on adjacent molecules ($\text{N}22\cdots\text{N}22$ $3.365(3)$ Å, $\text{N}22-\text{H}22\text{A}\cdots\text{N}22$ $2.65(4)$ Å, $\text{N}22-\text{H}22\text{A}\cdots\text{N}22$ $165(3)^\circ$).

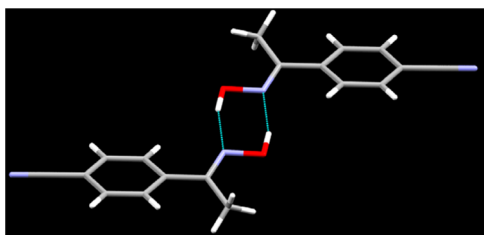
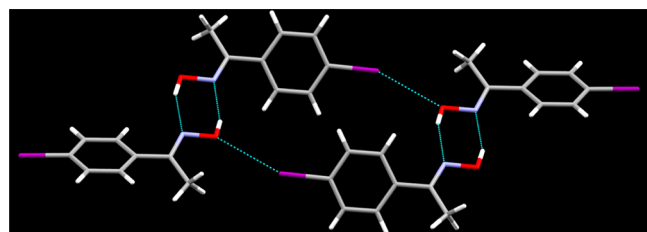


Figure 4. Dimer formation ($\text{R}_2^2(6)$) in the crystal structure of **2**.

Table 2. Key Geometric Parameters in the Crystal Structures of 2, 3, and 4

ligand	$d(\text{OH}\cdots\text{N})$ (Å)	$d(\text{HO}\cdots\text{N})$ (Å)	$\angle(\text{O}-\text{H}\cdots\text{N})$ (deg)	$d(\text{X}\cdots\text{O})^a$ (Å)	$\angle(\text{C}-\text{X}\cdots\text{O})^a$ (deg)
2	1.812(15)	2.7614(14)	160.5(15)		
3	1.998(19)	2.8379(16)	156.7(17)	3.0664(10)	152.29(4)
4	2.00(4)	2.813(3)	155(3)	3.1727(17)	154.37(7)

^aX = Br/I.Figure 5. Section of the crystal structure of 4 displaying hydrogen-bonded dimers ($R_2^2(6)$ motif) and $\text{I}\cdots\text{O}$ halogen bonds.

Of the 21 known crystal structures for amidoximes, fourteen (67%) contain dimers directed by $-\text{O}-\text{H}\cdots\text{N}$ interactions between adjacent oxime molecules (average $\text{HO}\cdots\text{N}$ bond distance and $\text{O}-\text{H}\cdots\text{N}$ bond angle is 2.77(4) Å and 145(7)° respectively) (Figure 8). Six of them (28%) are catemers, via $-\text{O}-\text{H}\cdots\text{N}$ hydrogen bonds (average $\text{HO}\cdots\text{N}$ bond distance and $\text{O}-\text{H}\cdots\text{N}$ bond angle is 2.75(7) Å and 171(8)°, respectively), and there is one case (5%) of catemer formation driven by $-\text{O}-\text{H}\cdots\text{O}$ interactions.

3.4. Cyano-Oximes ($\text{R}' = \text{CN}$). The crystal structure of 6 contains an infinite chain-of-rings ($R_4^4(34)$ motif), where each oxime molecule interacts with four adjacent molecules through

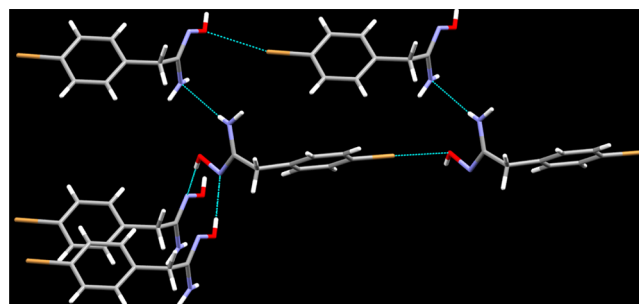
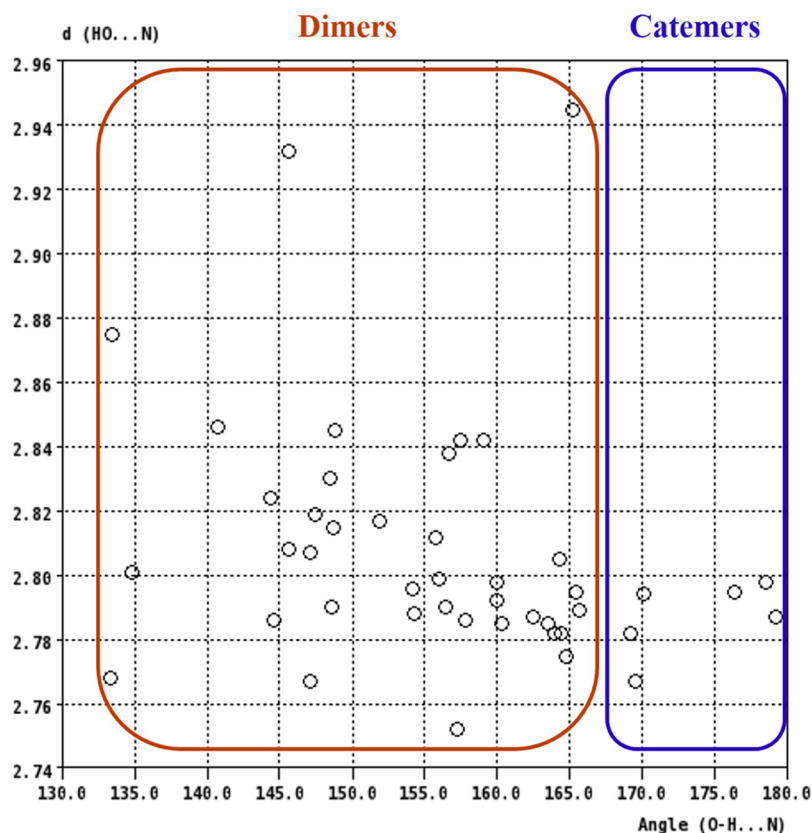


Figure 7. Section of the crystal structure of 5 displaying the three different types of intermolecular interactions.

$\text{O}-\text{H}\cdots\text{N}$ hydrogen bonds between the $\text{O}-\text{H}$ moiety and the nitrile nitrogen atom ($\text{O17}\cdots\text{N18}$ 2.7947(14) Å, $\text{O17}-\text{H17}\cdots\text{N18}$ 1.900(17) Å) (Figure 9).

The search for cyano-oximes by themselves in the CSD generated nine crystal structures, all of which contain $\text{O}-\text{H}\cdots\text{N}\equiv\text{C}$ hydrogen bonds between the oxime moiety and the nitrile nitrogen atom.

Figure 6. $\text{HO}\cdots\text{N}$ bond distance (Å) vs $\text{O}-\text{H}\cdots\text{N}$ bond angle (deg) for dimers and catemers of ketoximes.

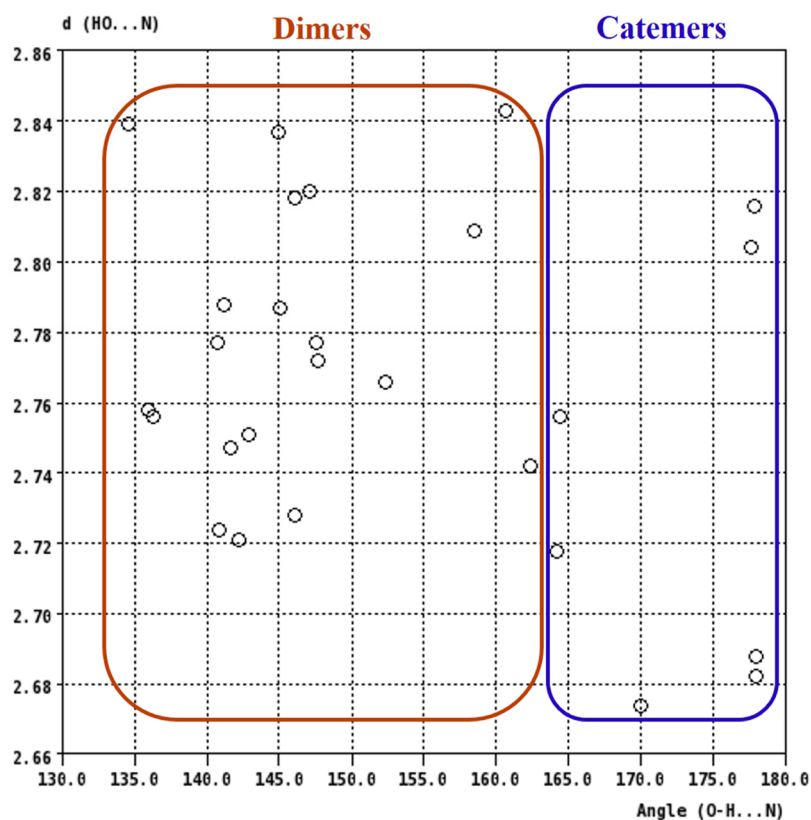


Figure 8. HO...N bond distance (Å) vs O-H...N bond angle (deg) for dimers and catemers of amidoximes.

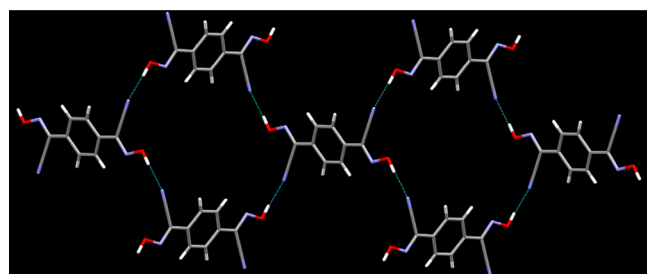


Figure 9. Section of the crystal structure of **6** displaying the infinite hydrogen-bonded chain-of-rings.

4. DISCUSSION

Six oximes have been synthesized and structurally characterized by single crystal X-ray diffraction to complement the existing data in the CSD to examine the structural chemistry of the four most common oximes in the solid state. Further, to fully understand the electronic or structural effects of the substituents (R') on the structures, the oximes can be grouped into four categories based on the specific structure-directing interactions present (Table 3).

The formation of dimers and O-H...N hydrogen-bonded catemers are only observed in three categories ($R' = -H$, $-CH_3$, $-NH_2$). Regardless of the substituent on these oximes, all dimers and O-H...N hydrogen-bonded catemers behave in a similar manner in terms of O-H...N bond distances (Å) and O-H...N bond angles (deg). The O-H...N bond angles (average value is 150°), in the case of all dimers, show that these hydrogen bonds are not completely linear, and thus highlights the relatively strained $R_2^2(6)$ motif which is formed in oxime dimers. In contrast, the hydrogen bonds in the C(3)

Table 3. Primary Motifs in Crystal Structures of Oximes

type of oxime	O-H...N $R_2^2(6)$ dimers	O-H...N C(3) catemers	O-H...O C(2) catemers	O-H...N≡ C C(6) catemers
aldoximes ($R' = H$)	42 (72%)	14 (24%)	2 (4%)	
ketoximes ($R' = CH_3$)	32 (87%)	5 (13%)	0 (0%)	
amidoximes ($R' = NH_2$)	14 (67%)	6 (28%)	1 (5%)	
cyano-oximes ($R' = CN$)	0 (0%)	0 (0%)	0 (0%)	9 (100%)

catemeric chains are closer to linear (average bond angle is 171°) and less constrained, as is expected with catemer formation.

The primary intermolecular interactions, whether they appear in dimers or catemers are very similar (two O-H...N interactions/two molecules) based on enthalpic considerations, but entropically catemer formation is favored over dimers.³² The greater number of dimers in the case of oximes can however be explained on the basis of three components of the "kinetic chelate effect":^{32,33} (i) the increased effective concentration of the tethered oxime moiety in dimers when compared to the second hydrogen-bonding molecule in catemers, (ii) the ease with which the tethered moiety can rotate and hydrogen-bond to form dimers, in comparison to the required second effective collision in catemers, and (iii) the lower rate of dissociation in dimers because, even if one hydrogen-bond breaks, a second one is still holding the moiety in place and consequently, they can quickly rejoin.

In such a case, we would expect to predominantly see $R_2^2(6)$ dimers for each category of oximes via O-H...N interactions

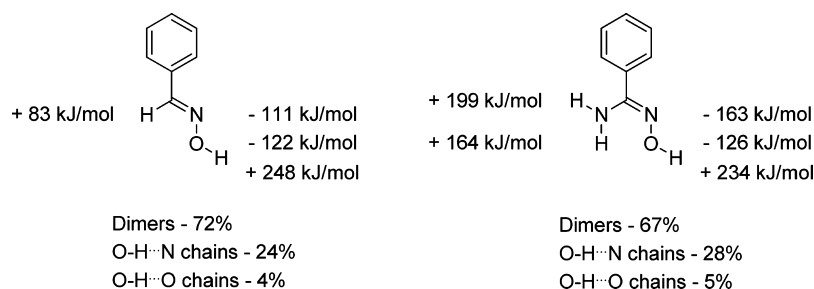


Figure 10. Molecular electrostatic potentials (MEPs) for aldoximes and amidoximes.

between two oxime moieties. However, when comparing the four types of oximes ($R' = -H, -CH_3, -NH_2, -CN$), aldoximes (24%) and amidoximes (28%) display a larger number of C(3) catemeric chains. This observation can be explained using molecular electrostatic potential charge calculations (MEPs) (Figure 10).

The common factor in aldoximes and amidoximes is the presence of an acidic proton ($R' = H, NH_2$) on the oxime moiety, which can potentially act as an alternative hydrogen-bond donor. Any such $C-H\cdots N/N-H\cdots N$ interaction between the substituent and the oxime nitrogen atom will hinder the formation of dimers, and thus increase the propensity for the formation of C(3) catemers, as seen in aldoximes and amidoximes.

In the case of ketoximes, there are two hydrogen-bond acceptors, the oxime nitrogen atom (-137 kJ/mol) and the oxime oxygen atom (-117 kJ/mol), of which the former is the better hydrogen-bond acceptor, as it has the higher charge (Figure 11). The presence of only one hydrogen-bond donor,

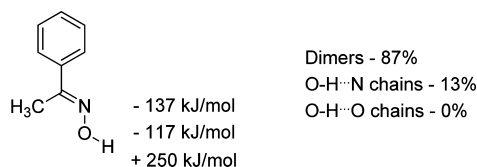


Figure 11. Molecular electrostatic potentials (MEPs) for ketoximes.

the $-O-H$ moiety ($+250$ kJ/mol), coupled with the absence of any interfering substituents on the oxime moiety, directs the ketoximes preferentially toward the formation of $R_2^2(6)$ dimers (87%) in the solid-state.

Two aldoximes (4%) form C(2) catemeric chains via $O-H\cdots O$ interactions, whereas none of the ketoximes do so. In the case of aldoximes, the electrostatic potential charges on the oxime nitrogen atom and oxygen atom are -111 and -122 kJ/mol respectively, hence the chances of catemer formation via the oxime oxygen atom increase because these values for the electrostatic potential charges are quite similar. In contrast, in ketoximes the electrostatic potential charge on the oxime nitrogen atom (-137 kJ/mol) is significantly greater than the charge on the oxygen atom (-117 kJ/mol), thus making the nitrogen atom the far better acceptor and hence catemer formation directed by $O-H\cdots O$ hydrogen-bonds is more unfavorable.

Cyano-oximes do not form any dimers or catemers, and this can again be rationalized using the MEPs (Figure 12). There are three potential hydrogen-bond acceptors in the case of the cyano-oxime moiety, with the nitrile nitrogen atom being the best acceptor, as it has the highest charge (-166 kJ/mol). Since

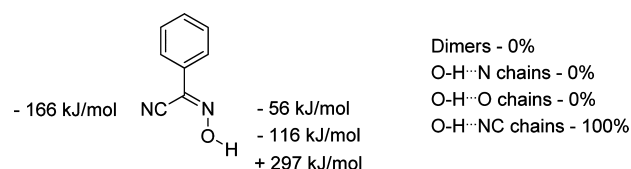


Figure 12. Molecular electrostatic potentials (MEPs) for cyano-oximes.

there is only one hydrogen-bond donor, the $-O-H$ moiety ($+297$ kJ/mol), we expect the primary electrostatic interaction to be the hydrogen bond between the $-O-H$ moiety and the nitrile nitrogen atom, which is the case for cyano-oximes (100%). This observation is consistent with earlier studies on nitriles based on pK_{HB} , wherein the nitrile moiety has been shown to be a competent hydrogen-bond acceptor.³⁴

The behavior of cyano-oximes is also supported by calculating the interaction-site pairing energies (ΔE in kJ) using the hydrogen-bond donor parameters (α_i), and the hydrogen-bond acceptor parameters (β_j), utilized by Hunter and co-workers (Figure 13).³⁵

The pairing energies for dimer formation (via $O-H\cdots N$ interactions) and for hydrogen bonding through the nitrile moiety in the case of cyano-oximes (Figure 13a) show a net benefit of $15-16$ kJ for the nitrile-based C(6) catemer, thus making it the more favorable interaction. Whereas, in the case of 2 the increased charge on the nitrogen atom of the oxime moiety, leads to a net benefit of only $10-11$ kJ in favor of hydrogen bonding via the nitrile moiety over the formation of dimers (Figure 13b). It seems that 2 prefers to form dimers in the solid-state via $O-H\cdots N$ interactions between the oxime moieties, which indicates that an 11 kJ advantage is not enough to break the kinetically favorable dimers, and thus lead to other interactions in the solid-state for oximes.

5. CONCLUSIONS

The available solid-state data in the CSD on the four major categories of oximes ($R' = -H, -CH_3, -NH_2, -CN$), complemented by six new relevant crystal structures, have provided the foundation for an examination of the structural chemistry and dominating intermolecular oxime...oxime hydrogen-bonding patterns present in the solid state. Aldoximes and amidoximes show the prevalence of a higher number of C(3) catemers, and this behavior can be explained by the presence of an acidic proton on the R' group, which may interfere with the formation of $R_2^2(6)$ dimers, thus resulting in a higher number of catemers. In the case of ketoximes, the higher charge on the oxime nitrogen atom, coupled with an inactive R' group, clearly tilts the balance toward the formation of $R_2^2(6)$ dimers. Cyano-oximes have a strong hydrogen-bond acceptor in the form of

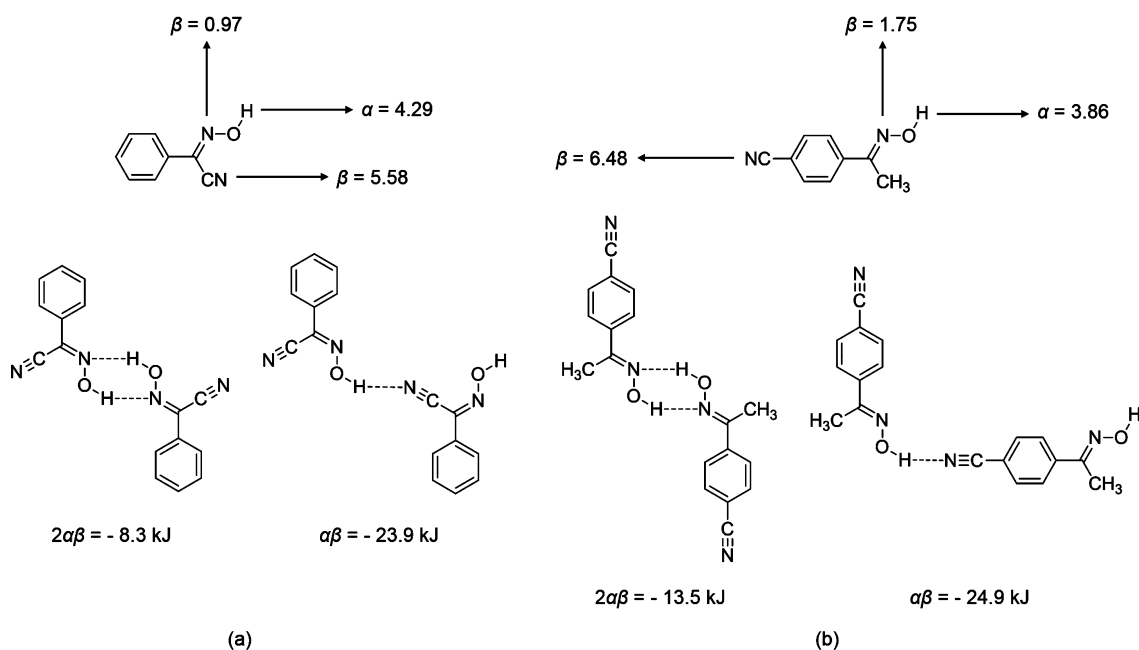


Figure 13. Calculated hydrogen-bond parameters α , β , and interaction-site pairing energies, for dimers, and O–H \cdots N \equiv C catemer for cyano-oximes (a) and for **2** (b).

the nitrile nitrogen atom, as shown by MEPs calculations and the interaction-site pairing energies, and thus only show O–H \cdots N \equiv C based C(6) catemers in the crystal lattice. In summary, it is noted that intermolecular homomeric oxime \cdots oxime interactions give rise to four distinct supramolecular synthons:^{9b} (i) R₂²(6) dimers, (ii) C(3) chains, (iii) C(2) chains, and (iv) C(6) chains. In view of their diverse structural chemistry, oximes may provide expanded supramolecular synthetic opportunities compared to other hydrogen-bonding moieties such as acids and amides, as it is possible to “fine tune” the directed assembly of oximes, by selecting the substituent (R') in such a way that a specific and desired solid-state architecture is obtained.

■ ASSOCIATED CONTENT

Supporting Information

Details of synthesis, characterization, and X-ray crystallography. This material is available free of charge via the Internet at <http://pubs.acs.org>.

■ AUTHOR INFORMATION

Corresponding Author

* E-mail: aakeroy@ksu.edu.

Notes

The authors declare no competing financial interest.

■ ACKNOWLEDGMENTS

We are grateful for financial support from the NSF (CHE-0957607) and from the Johnson Center for Basic Cancer Research.

■ REFERENCES

- (1) (a) Corey, E. J. *Angew. Chem., Int. Ed.* **2009**, *48*, 2100–2117. (b) Corey, E. J. *Angew. Chem., Int. Ed.* **2002**, *41*, 1650–1667.
- (2) Tiekink, E. R. T.; Vittal, J.; Zaworotko, M. *Organic Crystal Engineering: Frontiers in Crystal Engineering*, 1st ed.; Wiley, John & Sons, Inc.: Chichester, U.K., 2010.

- (3) Braga, D.; Grepioni, F. *Making Crystals by Design: Methods, Techniques and Applications*, 1st ed.; Wiley-VCH: Weinheim, Germany, 2006.

- (4) Desiraju, G. R.; Vittal, J. J.; Ramanan, A. *Crystal Engineering: A Textbook*; World Scientific Publishing Company, Inc.: Hackensack, NJ, 2011.

- (5) Aakeröy, C. B.; Champness, N. R.; Janiak, C. *CrystEngComm* **2010**, *12*, 22–43.

- (6) Herbstein, F. H. In *Comprehensive Supramolecular Chemistry*; MacNicol, D. D., Toda, F., Bishop, R., Eds.; Pergamon Press: New York, 1996; Vol. 6; pp 61–83.

- (7) (a) Hadzi, D.; Detoni, S. Hydrogen bonding in carboxylic acids and derivatives. In *Acid Derivatives*, Vol. 1; Patai, S., Ed.; John Wiley & Sons, Ltd.: Chichester, U.K., 1979. (b) Hamilton, W. C.; Ibers, J. A. *Hydrogen Bonding in Solids*; W. A. Benjamin: New York, 1968.

- (8) For a description of graph set notation for classifying hydrogen-bonding patterns, see: (a) Bernstein, J.; Davis, R. E.; Shimon, L.; Chang, N.-L. *Angew. Chem., Int. Ed. Engl.* **1995**, *34*, 1555–1573. (b) Etter, M. C. *Acc. Chem. Res.* **1990**, *23*, 120–126.

- (9) (a) Mareque Rivas, J. C.; Brammer, L. *New J. Chem.* **1998**, *22*, 1315–1318. (b) Desiraju, G. R. *Angew. Chem., Int. Ed. Engl.* **1995**, *34*, 2311–2327.

- (10) (a) Laurence, C.; Berthelot, M.; Graton, J. Hydrogen-Bonded Complexes of Phenols. In *Phenols*; Rappoport, Z., Ed.; John Wiley & Sons, Ltd.: Chichester, U.K., 2003. (b) Ermer, O.; Eling, A. *J. Chem. Soc., Perkin Trans. 2* **1994**, 925–944. (c) Bordwell, F. G.; McCallum, R. J.; Olmstead, W. N. *J. Org. Chem.* **1984**, *49*, 1424–1427.

- (11) (a) Eyer, P. A.; Worek, F. Oximes. In *Chemical Warfare Agents: Toxicology and Treatment*, 2nd ed.; Marrs, T. C., Maynard, R. L., Sidell, F. R., Eds.; John Wiley & Sons, Ltd.: Chichester, U.K., 2007. (b) Marsman, A. W.; Leusink, E. D.; Zwicker, J. W.; Jenneskens, L. W.; Smeets, W. J. J.; Veldman, N.; Spek, A. L. *Chem. Mater.* **1999**, *11*, 1484–1491.

- (12) Rappoport, Z.; Liebman, J. F. *The Chemistry of Hydroxylamines, Oximes and Hydroxamic Acids, Part 1*; Patai Series: The Chemistry of Functional Groups; John Wiley & Sons, Ltd.: Chichester, U.K., 2009.

- (13) (a) Aakeröy, C. B.; Salmon, D. J.; Smith, M. M.; Desper, J. *CrystEngComm* **2009**, *11*, 439–444. (b) Aakeröy, C. B.; Fasulo, M.; Schultheiss, N.; Desper, J.; Moore, C. *J. Am. Chem. Soc.* **2007**, *129*, 13772–13773. (c) Scarso, A.; Pellizzaro, L.; De Lucchi, O.; Linden, A.; Fabris, F. *Angew. Chem., Int. Ed.* **2007**, *46*, 4972–4975. (d) Mazik, M.;

- Bläser, D.; Boese, R. *Tetrahedron* **1999**, *55*, 7835–7840. (e) Burka, L. T. NTP Technical Report on the Toxicity Studies of Methyl Ethyl Ketoxime, 1999. http://ntp.niehs.nih.gov/ntp/htdocs/ST_rpts/tox051.pdf.
- (14) McGraw-Hill. Oxime, 2007. <http://books.mcgraw-hill.com/EST10/site/supparticles/Oxime-480600.pdf>.
- (15) Bertalosi, V.; Gilli, G.; Veronese, A. *Acta. Crystallogr., Sect. B.* **1982**, *B38*, 502–511.
- (16) Bruton, E. A.; Brammer, L.; Pigge, F. C.; Aakeröy, C. B.; Leinen, D. S. *New J. Chem.* **2003**, *27*, 1084–1094.
- (17) Low, J. N.; Santos, L. M. N. B. F.; Lima, C. F. R. A. C.; Brandão, P.; Gomes, L. R. *Eur. J. Chem.* **2010**, *1*, 61–66.
- (18) (a) Frutos, R. P.; Spero, D. M. *Tetrahedron Lett.* **1998**, *39*, 2475–2478. (b) Negi, S.; Matsukura, M.; Mizuno, M.; Miyake, K. *Synthesis* **1996**, *8*, 991–996. (c) Sasatani, S.; Miyazaki, T.; Maruoka, K.; Yamamoto, H. *Tetrahedron Lett.* **1983**, *24*, 4711–4712.
- (19) (a) Konidaris, K. F.; Katsoulakou, E.; Kaplanis, M.; Bekiari, V.; Terzis, A.; Raptopoulou, C. P.; Manessi-Zoupa, E.; Perlepes, S. P. *Dalton Trans.* **2010**, *39*, 4492–4494. (b) Chaudhuri, P.; Weyhermüller, T.; Wagner, R.; Khanra, S.; Biswas, B.; Bothe, E.; Bill, E. *Inorg. Chem.* **2007**, *46*, 9003–9016.
- (20) Allen, F. H. *Acta. Crystallogr., Sect. B.* **2002**, *B58*, 380–388.
- (21) CSD ConQuest 1.15; Cambridge Crystallographic Data Centre: Cambridge, U.K., 2012.
- (22) Aakeröy, C. B.; Sinha, A. S.; Epa, K. N.; Spartz, C. L.; Desper, J. *Chem. Commun.* **2012**, *48*, 11289–11291.
- (23) Aakeröy, C. B.; Sinha, A. S. *RSC Adv.* **2013**, DOI: 10.1039/C3RA40585K.
- (24) Prateetongkum, S.; Jovel, I.; Jackstell, R.; Vogl, N.; Weckbecker, C.; Beller, M. *Chem. Commun.* **2009**, *15*, 1990–1992.
- (25) Lyle, R. E.; Troschianiec, H. J. *J. Org. Chem.* **1955**, *20*, 1757–1760.
- (26) La Motta, C.; Sartini, S.; Salerno, S.; Simorini, F.; Taliani, S.; Marini, A.; Da Settimo, F.; Marinelli, L.; Limongelli, V.; Novellino, E. *J. Med. Chem.* **2008**, *51*, 3182–3193.
- (27) APEXII, version 2009.5-1; Bruker Analytical X-ray Systems: Madison, WI, 2009.
- (28) COSMO, version 1.60; Bruker Analytical X-ray Systems: Madison, WI; 1999–2009.
- (29) SAINT, version 7.60a; Bruker Analytical X-ray Systems: Madison, WI, 1997–2008.
- (30) SADABS, version 2008/1; Bruker Analytical X-ray Systems: Madison, WI, 2008.
- (31) SHELXTL, version 2008/4, Bruker Analytical X-ray Systems: Madison, WI, 2008.
- (32) Carter, M. J.; Beattie, J. K. *Inorg. Chem.* **1970**, *9*, 1233–1238.
- (33) Aakeröy, C. B.; Rajbanshi, A.; Desper, J. *Chem. Commun.* **2011**, *47*, 11411–11413.
- (34) (a) Le Questel, J.-Y.; Berthelot, M.; Laurence, C. *J. Chem. Soc., Perkin Trans. 2* **1997**, 2711–2718. (b) Berthelot, M.; Helbert, M.; Laurence, C.; Le Questel, J.-Y.; Anvia, F.; Taft, R. W. *J. Chem. Soc., Perkin Trans. 2* **1993**, 625–627.
- (35) (a) Musumeci, D.; Hunter, C. A.; Prohens, R.; Scuderi, S.; McCabe, J. F. *Chem. Sci.* **2011**, *2*, 883–890. (b) Hunter, C. A. *Angew. Chem., Int. Ed.* **2004**, *43*, 5310–5324.